Research Article

An ML-Based Estimate and the Cramer-Rao Bound for Data-Aided Channel Estimation in KSP-OFDM

Heidi Steendam, Marc Moeneclaey, and Herwig Bruneel

The Department of Telecommunications and Information Processing (TELIN), Ghent University,
Sint-Pietersnieuwstraat 41, 9000 Gent, Belgium

Correspondence should be addressed to Heidi Steendam, hs@telin.ugent.be

We consider the Cramer-Rao bound (CRB) for data-aided channel estimation for OFDM with known symbol padding (KSP-OFDM). The pilot symbols used to estimate the channel are positioned not only in the guard interval but also on some of the OFDM carriers, in order to improve the estimation accuracy for a given guard interval length. As the true CRB is very hard to evaluate, we derive an approximate analytical expression for the CRB, that is, the Gaussian CRB (GCRB), which is accurate for large block sizes. This derivation involves an invertible linear transformation of the received samples, yielding an observation vector of which a number of components are (nearly) independent of the unknown information-bearing data symbols. The low SNR limit of the GCRB is obtained by ignoring the presence of the data symbols in the received signals. At high SNR, the GCRB is mainly determined by the observations that are (nearly) independent of the data symbols; the additional information provided by the other observations is negligible. Both SNR limits are inversely proportional to the SNR. The GCRB is essentially independent of the FFT size and the used pilot sequence, and inversely proportional to the number of pilots. For a given number of pilot symbols, the CRB slightly increases with the guard interval length. Further, a low complexity ML-based channel estimator is derived from the observation subset that is (nearly) independent of the data symbols. Although this estimator exploits only a part of the observation, its mean-squared error (MSE) performance is close the CRB for a large range of SNR. However, at high SNR, the MSE reaches an error floor caused by the residual presence of data symbols in the considered observation subset.

1. INTRODUCTION

Multicarrier systems have received considerable attention for high data rate communications [1] because of their robustness to channel dispersion. To cope with channel dispersion, the multicarrier system inserts between blocks of data a guard interval, with a length larger than the channel impulse response. The most commonly used types of guard interval are cyclic prefix, zero padding, and known symbol padding. In cyclic prefix OFDM, the guard interval consists of a cyclic extension of the data block whereas in zero-padding OFDM, no signal is transmitted during the guard interval [2]. In OFDM with known symbol padding, (KSP-OFDM), which is considered in this paper, the guard interval consists of a number of known samples [3–5]. One of the advantages of KSP-OFDM as compared to CP-OFDM and ZP-OFDM is its improved timing synchronization ability: in CP-OFDM

and ZP-OFDM, low complexity timing synchronization algorithms like the Schmidl-Cox [6] algorithm, typically result in an ambiguity of the timing estimate over the length of the guard interval, whereas in KSP-OFDM, low complexity timing synchronization algorithms can be found avoiding this ambiguity problem by properly selecting the samples of the guard interval [7].

In KSP-OFDM, the known samples from the guard interval can serve as pilot symbols to obtain a data-aided estimate of the channel. However, as the length of the guard interval is typically small as compared to the FFT length (to keep the efficiency of the multicarrier system as high as possible) the number of known samples is typically too small to obtain an accurate channel estimate. To improve the channel estimation accuracy, the number of pilot symbols must be increased. This can be done by increasing the guard interval length or by keeping the length of the guard interval constant

and replacing in the data part of the signal some data carriers by pilot carriers. As the former strategy results in a stronger reduction of the OFDM system efficiency than the latter [8], the latter strategy will be considered.

In this paper, we derive an approximative analytical expression for the Gaussian Cramer-Rao bound (GCRB) for channel estimation when the pilot symbols are distributed over the guard interval and pilot carriers. The paper is organized as follows. In Section 2, we describe the system and determine the GCRB. Further, we derive a low complexity ML-based estimate for the channel in Section 3. Numerical results are given in Section 4 and the conclusions are drawn in Section 5.

2. SYSTEM MODEL AND CRAMER-RAO BOUND

2.1. System model

In KSP-OFDM, the data symbols to be transmitted are grouped into blocks of N symbols: the ith symbol block is denoted $\mathbf{a}_i = (a_i(0), \ldots, a_i(N-1))^T$. As explained below, $\mathbf{a}_i$ contains information-bearing data symbols and pilot symbols. The symbols $\mathbf{a}_i$ are then modulated on the OFDM carriers using an N-point inverse FFT. The guard interval, consisting of ν known samples, is inserted after each OFDM symbol (this corresponds to the dark-gray area in Figure 1(a)), resulting in $N + \nu$ time-domain samples $\mathbf{s}_i$ during block i:

$$\mathbf{s}_i = \sqrt{\frac{N}{N+\nu}}\begin{pmatrix} \mathbf{F}^+\mathbf{a}_i \\ \mathbf{b}_g \end{pmatrix}, \qquad (1)$$

where $\mathbf{F}$ is the $N \times N$ matrix corresponding to the FFT operation, that is, $\mathbf{F}_{k,\ell} = (1/\sqrt{N})e^{-j2\pi(k\ell/N)}$, and $\mathbf{b}_g = (b_g(0), \ldots, b_g(\nu-1))^T$ corresponds to the ν known samples of the guard interval.

The sequence (1) is transmitted over a dispersive channel with L taps $\mathbf{h} = (h(0), \ldots, h(L-1))^T$ and disturbed by additive white Gaussian noise $\mathbf{w}$. The zero-mean noise components $w(k)$ have variance N_0. To avoid interference between symbols from neighboring blocks, we assume that the duration of the guard interval exceeds the duration of the channel impulse length, that is, $\nu \geq L - 1$. Without loss of generality, we consider the detection of the OFDM block with index $i = 0$, and drop the block index for notational convenience. Taking the condition $\nu \geq L - 1$ into account, the corresponding $N + \nu$ received time-domain samples can be written as

$$\mathbf{r} = \mathbf{H}_{\mathrm{ch}}\mathbf{s} + \mathbf{w}, \qquad (2)$$

where $(\mathbf{H}_{\mathrm{ch}})_{k,k'} = h(k - k')$ is the $(N + \nu) \times (N + \nu)$ channel matrix. For data detection, the known samples are first subtracted from the received signal. Then, the ν samples of the guard interval are added to the first ν samples of the data part of the block, as shown in Figure 1(b), and an FFT is applied to the resulting N samples. As the known samples are distorted by the channel (as can be seen in Figure 1(b)), the channel needs to be known before the contribution from the known samples can be removed from the received signal.

To estimate the channel, we assume that M pilot symbols are available. As we select the length of the guard interval in function of the channel impulse length and not in function of the precision of the estimation, only ν of the M pilot symbols can be placed in the guard interval. This implies that $M - \nu$ carriers in (1) must contain pilot symbols, which are denoted by $\mathbf{b}_c = (b_c(0), \ldots, b_c(M-\nu-1))^T$. We define I_p and I_d as the sets of carriers modulated by the pilot symbols and the data symbols, respectively, with $I_p \cup I_d = \{0, \ldots, N-1\}$. Hence, the symbol vector $\mathbf{a}$ contains $M - \nu$ pilot symbols $\mathbf{b}_c$ and $N + \nu - M$ data symbols which are denoted by $\mathbf{a}_d$. We assume that the data symbols are independent identically distributed (i.i.d.) with $E[|a_d(n)|^2] = E_s$ and the pilot symbols are selected such that $E[|b_g(m)|^2] = E[|b_c(n)|^2] = E_s$. The normalization factor $\sqrt{N/(N+\nu)}$ in (1) then gives rise to $E[|s(m)|^2] = E_s$. It can easily be verified that the observation of the $N + \nu$ time-domain samples corresponding to one OFDM block (as shown in Figure 1(c)) contains sufficient information to estimate $\mathbf{h}$. Rewriting (2), we obtain

$$\mathbf{r} = \mathbf{B}\mathbf{h} + \tilde{\mathbf{w}}, \qquad (3)$$

where $\mathbf{B} = \mathbf{B}_g + \mathbf{B}_c$ is a $(N+\nu) \times L$ matrix. The matrix $\mathbf{B}_g$ contains the contributions from the pilot symbols in the guard interval, and is given by

$$(\mathbf{B}_g)_{k,\ell} = \sqrt{\frac{N}{N+\nu}}b_g(|k - \ell + \nu|_{N+\nu}), \qquad (4)$$

where $|x|_K$ is the modulo-K operation of x yielding a result in the interval $[0, K[$, and $b_g(k) = 0$ for $k \geq \nu$. The matrix $\mathbf{B}_c$ consists of the contributions from the pilots transmitted on the carriers, where

$$(\mathbf{B}_c)_{k,\ell} = \sqrt{\frac{N}{N+\nu}}s_p(k - \ell). \qquad (5)$$

The vector $\mathbf{s}_p$ equals the N-point IFFT of the pilot carriers only, that is, $\mathbf{s}_p = \mathbf{F}_p\mathbf{b}_c$. The $N \times (M - \nu)$ matrix $\mathbf{F}_p$ consists of a subset of columns of the IFFT matrix $\mathbf{F}^+$ corresponding to the set I_p of pilot carriers. Note that $s_p(k) = 0$ for $k < 0$ or $k \geq N$. The disturbance in (3) can be written as

$$\tilde{\mathbf{w}} = \mathbf{H}\mathbf{F}_d\mathbf{a}_d + \mathbf{w} = \mathbf{H}\mathbf{s}_d + \mathbf{w}, \qquad (6)$$

where $\mathbf{H}_{k,\ell} = h(k - \ell)$ is a $(N + \nu) \times N$ matrix. The $N \times (N + \nu - M)$ matrix $\mathbf{F}_d$ consists of a subset of columns of $\mathbf{F}^+$ corresponding to the set I_d of data carriers. Hence, $\mathbf{s}_d = \mathbf{F}_d\mathbf{a}_d$ equals the N-point IFFT of the data carriers symbols only, that is, the contribution from the data symbols to the received time-domain samples $\mathbf{r}$.

2.2. Gaussian Cramer-Rao bound

First, let us determine the Cramer-Rao bound of the estimation of $\mathbf{h}$ from the observation $\mathbf{r}$. The Cramer-Rao bound is defined by $\mathbf{R}_{\mathbf{h}-\hat{\mathbf{h}}} - \mathbf{J}^{-1} \geq 0$ [9], where $\mathbf{R}_{\mathbf{h}-\hat{\mathbf{h}}}$ is the autocorrelation matrix of the estimation error $\mathbf{h} - \hat{\mathbf{h}}$, $\hat{\mathbf{h}}$ is an estimate of $\mathbf{h}$, and the Fisher information matrix $\mathbf{J}$ is defined as

$$\mathbf{J} = E_\mathbf{r}\left[\left(\frac{\partial}{\partial \mathbf{h}}\ln p(\mathbf{r} \mid \mathbf{h})\right)^+ \left(\frac{\partial}{\partial \mathbf{h}}\ln p(\mathbf{r} \mid \mathbf{h})\right)\right]. \qquad (7)$$
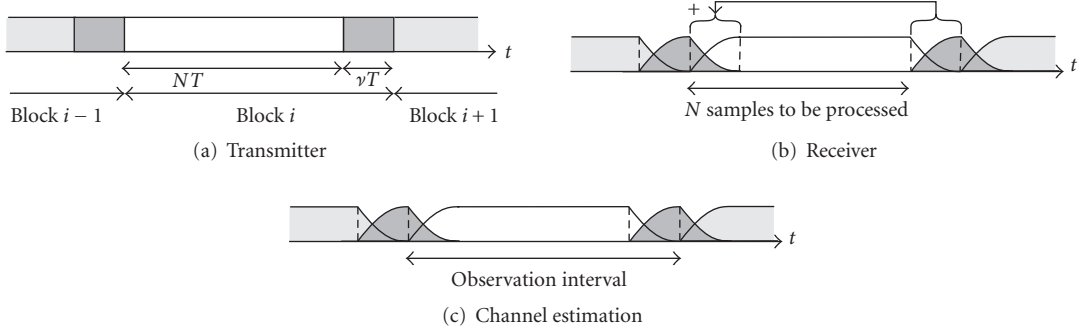
FIGURE 1: Time-domain signal of KSP-OFDM: (a) transmitted signal, (b) received signal and observation interval for data detection, and (c) observation interval for channel estimation.

Hence, the MSE of an estimator is lower bounded by $E[\|\mathbf{h} - \hat{\mathbf{h}}\|^2] = \text{trace}(\mathbf{R}_{\mathbf{h}-\hat{\mathbf{h}}}) \geq \text{trace}(\mathbf{J}^{-1})$. In our analysis, we assume that $\mathbf{s}_d = \mathbf{F}_d\mathbf{a}_d$ is zero-mean Gaussian distributed; this yields a good approximation for large $N + \nu - M$ (say for large block sizes) and results in the Gaussian CRB (GCRB). In this case, $\mathbf{r}$ given $\mathbf{h}$ is Gaussian distributed, that is, $\mathbf{r} \mid \mathbf{h} \sim N(\mathbf{Bh}, \mathbf{R}_{\tilde{\mathbf{w}}})$, where $\mathbf{R}_{\tilde{\mathbf{w}}} = E_s(N/(N+\nu))\mathbf{HF}_d\mathbf{F}_d^{+}\mathbf{H}^{+} + N_0\mathbf{I}_{N+\nu}$ is the autocorrelation matrix of the disturbance $\tilde{\mathbf{w}}$ and $\mathbf{I}_K$ is the $K \times K$ identity matrix. Hence, it follows that

$$\ln p(\mathbf{r} \mid \mathbf{h}) = C - \frac{1}{2}\ln [\![\mathbf{R}_{\tilde{\mathbf{w}}}]\!] - (\mathbf{r} - \mathbf{Bh})^{+}\mathbf{R}_{\tilde{\mathbf{w}}}^{-1}(\mathbf{r} - \mathbf{Bh}), \tag{8}$$

where C is an irrelevant constant and $[\![\mathbf{R}_{\tilde{\mathbf{w}}}]\!]$ is the determinant of $\mathbf{R}_{\tilde{\mathbf{w}}}$. Note that as the autocorrelation matrix $\mathbf{R}_{\tilde{\mathbf{w}}}$ depends on the channel taps $\mathbf{h}$ to be estimated, we need the derivative of $[\![\mathbf{R}_{\tilde{\mathbf{w}}}]\!]$ and $\mathbf{R}_{\tilde{\mathbf{w}}}^{-1}$ with respect to $\mathbf{h}$ to obtain the Fisher information matrix, and hence the GCRB. As in general these derivatives are difficult to obtain, the computation of the GCRB is in general very complex. In order to find an analytical expression for the GCRB and avoid the difficulty of finding the derivatives of $[\![\mathbf{R}_{\tilde{\mathbf{w}}}]\!]$ and $\mathbf{R}_{\tilde{\mathbf{w}}}^{-1}$ for a general autocorrelation matrix $\mathbf{R}_{\tilde{\mathbf{w}}}$, we suggest the following approach.

Let us consider the approximation of the data contribution $\mathbf{HF}_d\mathbf{a}_d$ in (6) by $\tilde{\mathbf{F}}\tilde{\mathbf{H}}\mathbf{a}_d$, where the matrix $\tilde{\mathbf{F}}_{k,\ell} = (1/\sqrt{N})e^{j2\pi(kn_\ell/N)}$, $\tilde{\mathbf{H}}$ is a diagonal matrix with diagonal elements H_{n_ℓ}, $n_\ell \in I_d$ and

$$H_m = \sum_{k=0}^{N-1} h(k)e^{-j2\pi(km/N)}. \tag{9}$$

In this approximation, we have neglected, in the contribution from $\mathbf{a}_d$ to $\mathbf{r}$, the transient at the edges of the received block; this approximation is valid for long blocks, that is, when $N \gg \nu$. When applying an invertible linear transformation that is independent of the parameter to be estimated, to the observation $\mathbf{r}$, this will have no effect on the CRB. Further, note that $\tilde{\mathbf{H}}\mathbf{a}_d$ contains only $N + \nu - M < N + \nu$ components. Therefore, it is possible to find an invertible linear transformation $\mathbf{T}$ that maps $\mathbf{r}$ to an $(N + \nu) \times 1$ vector $\mathbf{r}' = [\mathbf{r}_1^T \mathbf{r}_2^T]^T$, where $\mathbf{r}_1$ depends on the transmitted data symbols $\mathbf{a}_d$ and $\mathbf{r}_2$ is independent of $\mathbf{a}_d$. This transform can

be found by performing the QR-decomposition of the matrix $\tilde{\mathbf{F}}$, that is, $\tilde{\mathbf{F}} = \mathbf{QV}$, where $\mathbf{Q}$ is a $(N+\nu) \times (N+\nu)$ unitary matrix $\mathbf{Q}^{+} = \mathbf{Q}^{-1}$ and

$$\mathbf{V} = \begin{pmatrix} \mathbf{U} \\ \mathbf{0} \end{pmatrix}, \tag{10}$$

where $\mathbf{U}$ is an upper triangular matrix. Taking into account that $\tilde{\mathbf{F}}$ has dimension $(N+\nu) \times (N+\nu-M)$, it follows that $\tilde{\mathbf{F}}$ (and thus $\mathbf{V}$) has rank $N + \nu - M$. Hence, $\mathbf{V}$ contains M zero rows, that is, $\mathbf{U}$ is a $(N+\nu-M) \times (N+\nu-M)$ matrix and the all zero matrix $\mathbf{0}$ in (10) has dimension $M \times (N+\nu-M)$. The transform matrix $\mathbf{T}$ is then given by $\mathbf{T} = \mathbf{Q}^{+}$, and the resulting observations yield

$$\mathbf{r}' = \mathbf{Tr} = \begin{pmatrix} \mathbf{r}_1 \\ \mathbf{r}_2 \end{pmatrix} = \begin{pmatrix} \mathbf{B}_1 \\ \mathbf{B}_2 \end{pmatrix}\mathbf{h} + \begin{pmatrix} \mathbf{U} \\ \mathbf{0} \end{pmatrix}\tilde{\mathbf{H}}\mathbf{a}_d + \begin{pmatrix} \mathbf{w}_1 \\ \mathbf{w}_2 \end{pmatrix}. \tag{11}$$

In (11), $\mathbf{B}_1$ and $\mathbf{B}_2$ correspond to the first $N+\nu-M$ and last M rows of $\mathbf{TB}$, respectively. Because of the unitary nature of the matrix $\mathbf{T}$, the noise contributions $\mathbf{w}_1$ and $\mathbf{w}_2$ are statistically independent and have the same mean and variance as the noise $\mathbf{w}$.

We now compute the GCRB related to the estimation of the channel taps $\mathbf{h}$ based on the observation $\mathbf{r}' = \mathbf{Tr}$ using the approximation $\mathbf{HF}_d = \tilde{\mathbf{F}}\tilde{\mathbf{H}}$. The observation $\mathbf{r}'$ given $\mathbf{h}$ is also Gaussian distributed, that is, $\mathbf{r}' \mid \mathbf{h} \sim N(\mathbf{TBh}, \mathbf{R}_{\mathbf{w}'})$, where $\mathbf{R}_{\mathbf{w}'}$ is the autocorrelation matrix of the disturbance $\mathbf{w}' = \mathbf{T}\tilde{\mathbf{w}}$ and is given by

$$\mathbf{R}_{\mathbf{w}'} = \begin{pmatrix} \mathbf{R}_1 & \mathbf{0} \\ \mathbf{0} & \mathbf{R}_2 \end{pmatrix}, \tag{12}$$

where $\mathbf{R}_1 = E_s(N/(N+\nu))\mathbf{U}\tilde{\mathbf{H}}\tilde{\mathbf{H}}^{+}\mathbf{U}^{+} + N_0\mathbf{I}_{N+\nu-M}$ and $\mathbf{R}_2 = N_0\mathbf{I}_M$. As $\mathbf{r}_1$ and $\mathbf{r}_2$ given $\mathbf{h}$ are statistically independent, it can easily be verified that the Fisher information matrix is given by $\mathbf{J} = \mathbf{J}_1 + \mathbf{J}_2$, where

$$\mathbf{J}_i = E_{\mathbf{r}_i}\left[\left(\frac{\partial}{\partial \mathbf{h}}\ln p(\mathbf{r}_i \mid \mathbf{h}) \right)^{+} \left(\frac{\partial}{\partial \mathbf{h}}\ln p(\mathbf{r}_i \mid \mathbf{h}) \right) \right] \tag{13}$$

with $i = 1, 2$; and

$$\ln p(\mathbf{r}_i \mid \mathbf{h}) = C - \frac{1}{2}\ln [\![\mathbf{R}_i]\!] - (\mathbf{r}_i - \mathbf{B}_i\mathbf{h})^{+}\mathbf{R}_i^{-1}(\mathbf{r}_i - \mathbf{B}_i\mathbf{h}). \tag{14}$$

We now compute the Fisher information matrices $\mathbf{J}_1$ and $\mathbf{J}_2$, separately. First, we determine $\mathbf{J}_2$. As the observation $\mathbf{r}_2 = \mathbf{B}_2\mathbf{h} + \mathbf{w}_2$ is independent of the data symbols, and $p(\mathbf{r}_2 \mid \mathbf{h}) \sim N(\mathbf{B}_2\mathbf{h}, N_0\mathbf{I}_M)$, where $\mathbf{B}_2$ is independent of $\mathbf{h}$, it can easily be found that

$$\mathbf{J}_2 = \frac{1}{N_0}\mathbf{B}_2^+\mathbf{B}_2. \tag{15}$$

Note that the CRB of an estimation can not increase by using more observations. Hence, the GCRB obtained from the observation $\mathbf{r}_2$ only is an upper bound for the GCRB obtained from the whole observation $\mathbf{r}'$.

Next, we determine $\mathbf{J}_1$, based on the observation $\mathbf{r}_1 = \mathbf{B}_1\mathbf{h} + \mathbf{U}\widetilde{\mathbf{H}}\mathbf{a}_d + \mathbf{w}_1$ only. Note that, although $\mathbf{B}_1$ is independent of $\mathbf{h}$, the autocorrelation matrix $\mathbf{R}_1$ of the disturbance $\mathbf{U}\widetilde{\mathbf{H}}\mathbf{a}_d + \mathbf{w}_1$ is not. Recall that to compute $\mathbf{J}_1$, we need the derivative of $[\![\mathbf{R}_1]\!]$ and $(\mathbf{R}_1)^{-1}$ with respect to $\mathbf{h}$. These derivatives can be written in an analytical form using the following approximation: when $M - \nu \ll N$, $\widetilde{\mathbf{F}}\widetilde{\mathbf{F}}^+$ can be approximated by the identity matrix $\mathbf{I}_{N+\nu-M}$. When this assumption holds, $\mathbf{R}_1$ can be written as

$$\mathbf{R}_1 = \mathbf{T}_1\widetilde{\mathbf{F}}\Delta\widetilde{\mathbf{F}}^+\mathbf{T}_1^+, \tag{16}$$

where $\mathbf{T}_1$ consists of the $N + \nu - M$ first rows of $\mathbf{T}$, and Δ is a diagonal matrix with elements α_ℓ defined as

$$\alpha_\ell = N_0 + \frac{N}{N+\nu}E_s|H_{n_\ell}|^2, \quad n_\ell \in I_d. \tag{17}$$

Because $\widetilde{\mathbf{F}}$ has rank $N+\nu-M$, $\mathbf{T}_1\widetilde{\mathbf{F}}$ is a full-rank square matrix. When $\mathbf{A}$ and $\mathbf{B}$ are square matrices, it follows that $[\![\mathbf{AB}]\!] = [\![\mathbf{A}]\!][\![\mathbf{B}]\!]$. Hence, $\ln[\![\mathbf{R}_1]\!]$ reduces to

$$\ln[\![\mathbf{R}_1]\!] = \ln[\![\mathbf{T}_1\widetilde{\mathbf{F}}\widetilde{\mathbf{F}}^+\mathbf{T}_1^+]\!] + \sum_{n_\ell \in I_d}\ln(\alpha_\ell). \tag{18}$$

Further, as $\mathbf{T}_1\widetilde{\mathbf{F}}$ has full rank, the inverse of $\mathbf{R}_1$ (16) can easily be computed:

$$(\mathbf{R}_1)^{-1} = (\widetilde{\mathbf{F}}^+\mathbf{T}_1^+)^{-1}\Delta^{-1}(\mathbf{T}_1\widetilde{\mathbf{F}})^{-1}. \tag{19}$$

Using (18) and (19), the derivate of $\ln[\![\mathbf{R}_1]\!]$ and $(\mathbf{R}_1)^{-1}$ with respect to $\mathbf{h}$ can easily be computed. Defining

$$\gamma_{k,\ell} = \frac{N}{N+\nu}E_s H_{n_\ell}^* e^{-j2\pi(kn_\ell/N)},$$
$$\beta_k = -\frac{1}{2}\sum_{n_\ell \in I_d}\frac{\gamma_{k,\ell}}{\alpha_\ell}, \tag{20}$$

it follows after tedious but straightforward computations (see the appendix) that the Fisher information matrix $\mathbf{J}_1$ is given by

$$(\mathbf{J}_1)_{k,k'} = (\mathbf{B}_1^+\mathbf{R}_1^{-1}\mathbf{B}_1)_{k,k'} + \beta_k^*\beta_{k'} + \sum_{n_\ell \in I_d}\frac{\gamma_{k,\ell}^*\gamma_{k',\ell}}{|\alpha_\ell|^2}. \tag{21}$$

Combining (15) and (21), the total Fisher information matrix, based on the observation of both $\mathbf{r}_1$ and $\mathbf{r}_2$, is given by (see the appendix)

$$(\mathbf{J})_{k,k'} = (\mathbf{B}^+\mathbf{R}_{\widetilde{\mathbf{w}}}^{-1}\mathbf{B})_{k,k'} + \beta_k^*\beta_{k'} + \sum_{n_\ell \in I_d}\frac{\gamma_{k,\ell}^*\gamma_{k',\ell}}{|\alpha_\ell|^2}. \tag{22}$$

Let us now consider the behavior of the GCRB for low and high values of E_s/N_0. When $E_s/N_0 \ll 1$, it follows from (17), (20) that the second and third term in (22) are proportional to $(E_s/N_0)^2$, whereas it can be verified from the definitions of $\mathbf{B}$ and $\mathbf{R}_{\widetilde{\mathbf{w}}}$ that the first term in (22) is proportional to E_s/N_0. Hence, the first term in (22) is dominant at low E_s/N_0 and the GCRB reduces to CRB $=$ trace $[(\mathbf{B}^+\mathbf{R}_{\widetilde{\mathbf{w}}}^{-1}\mathbf{B})^{-1}]$. Taking into account that at low E_s/N_0 the autocorrelation matrix $\mathbf{R}_{\widetilde{\mathbf{w}}}$ reduces to $N_0\mathbf{I}_{N+\nu}$, the low SNR limit of the GCRB equals trace $(N_0(\mathbf{B}^+\mathbf{B})^{-1})$, which is inversely proportional to E_s/N_0. This low SNR limit equals the GCRB that results from ignoring the data symbols $\mathbf{a}_d$ in (6); this limit corresponds to the low SNR limit of the true CRB that has been derived in [8]. To evaluate the low E_s/N_0 limit of the (G)CRB, we approximate $\mathbf{B}^+\mathbf{B}$ by its average over all possible pilot sequences, that is, $\overline{\mathbf{B}^+\mathbf{B}} = E[\mathbf{B}^+\mathbf{B}]$. We assume that the pilot symbols are selected in a pseudorandom way. In that case, $E[\mathbf{B}^+\mathbf{B}]$ is essentially equal to $E[\mathbf{B}^+\mathbf{B}] = E[\mathbf{B}_g^+\mathbf{B}_g] + E[\mathbf{B}_c^+\mathbf{B}_c]$. The components of the first term $E[\mathbf{B}_g^+\mathbf{B}_g]$ are given by

$$E[(\mathbf{B}_g^+\mathbf{B}_g)_{k,k'}]$$
$$= \frac{N}{N+\nu}\sum_{\ell=0}^{\nu-1}E[b_g^*(|\ell-k+\nu|_{N+\nu})b_g(|\ell-k'+\nu|_{N+\nu})]$$
$$= \frac{N}{N+\nu}\sum_{\ell=0}^{\nu-1}E_s\delta_{k,k'} = \frac{N}{N+\nu}\nu E_s\delta_{k,k'}. \tag{23}$$

The components of the second term $E[\mathbf{B}_c^+\mathbf{B}_c]$ are given by

$$E[(\mathbf{B}_c^+\mathbf{B}_c)_{k,k'}]$$
$$= \frac{N}{N+\nu}\sum_{\ell=0}^{N-1}E[s_p^*(\ell-k)s_p(\ell-k')]$$
$$= \frac{N}{N+\nu}\sum_{\ell=0}^{N-1}\sum_{m,m'\in I_p}\frac{1}{N}E[b_c^*(m)b_c(m')]$$
$$\cdot e^{-j2\pi((\ell-k)m/N)}e^{j2\pi((\ell-k')m'/N)}$$
$$= \frac{N}{N+\nu}E_s\sum_{\ell=0}^{N-1}\sum_{m\in I_p}\frac{1}{N}e^{j2\pi((k-k')m/N)}$$
$$\approx \frac{N}{N+\nu}(M-\nu)E_s\delta_{k,k'}. \tag{24}$$

When the pilot symbols are evenly distributed over the carriers (i.e., the set I_p of pilot carriers is given by $I_p = \{n_0 + m\epsilon \mid m = 0,\ldots,M-\nu-1\}$, where n_0 belongs to the set $\{0,\ldots,\rho\}$, with $\rho = (N-1) - (M-\nu-1)\epsilon$, $\epsilon =$ floor$(N/(M-\nu))$) and $M-\nu$ divides N, the approximation in the last line in (24) turns into an equality. Taking into account (23) and (24), $E[\mathbf{B}^+\mathbf{B}]$ can be approximated by $E[\mathbf{B}^+\mathbf{B}] = (N/(N+\nu))ME_s\mathbf{I}_L$, from which it follows that the low E_s/N_0 limit of the (G)CRB reduces to CRB $= (L/M)((N/(N+\nu))(E_s/N_0))^{-1}$. Hence, the low E_s/N_0 limit of the (G)CRB is inversely proportional to the number of pilot symbols M.

When $E_s/N_0 \gg 1$, it follows from (17), (20) that the second and third term in (22) become independent of E_s/N_0.

Further, if we split the first term of (22) as $\mathbf{B}^+\mathbf{R}_{\widetilde{\mathbf{w}}}^{-1}\mathbf{B} = \mathbf{B}_1^+\mathbf{R}_1^{-1}\mathbf{B}_1 + (1/N_0)\mathbf{B}_2^+\mathbf{B}_2$ (see the appendix), it can be verified from the definitions of $\mathbf{B}_1$, $\mathbf{B}_2$, and $\mathbf{R}_1$ that the first term $\mathbf{B}_1^+\mathbf{R}_1^{-1}\mathbf{B}_1$ is independent of E_s/N_0 and the second term $(1/N_0)\mathbf{B}_2^+\mathbf{B}_2$ is proportional to E_s/N_0 at high E_s/N_0. Hence, the Fisher information matrix at high E_s/N_0 is dominated by the term $(1/N_0)\mathbf{B}_2^+\mathbf{B}_2$ so the high SNR limit of the GCRB equals CRB = trace $[N_0(\mathbf{B}_2^+\mathbf{B}_2)^{-1}]$, which is inversely proportional to E_s/N_0. This high SNR limit equals the GCRB corresponding to $\mathbf{J}_2^{-1}$, which corresponds to exploiting for channel estimation only the observations $\mathbf{r}_2$ that are independent of the data symbols. This indicates that at high SNR, the information contained in the observations $\mathbf{r}_1$, that are affected by the data symbols can be neglected as compared to the information provided by $\mathbf{r}_2$. Based on this finding, we will derive in Section 3 a channel estimator that only makes use of the observations $\mathbf{r}_2$.

Finally, note that both the low and high E_s/N_0 limits of the GCRB are independent of $\mathbf{h}$.

3. THE SUBSET ESTIMATOR

The ML estimate of a vector $\mathbf{h}$ from an observation $\mathbf{z}$ is defined as [9]:

$$\hat{\mathbf{h}}_{\text{ML}} = \arg\max_{\mathbf{h}} p(\mathbf{z} \mid \mathbf{h}). \tag{25}$$

In the previous section, we have found that all observations were linear in the parameter $\mathbf{h}$ to be estimated: $\mathbf{z} = \mathbf{A}\mathbf{h} + \boldsymbol{\omega}$, where $\boldsymbol{\omega}$ is zero-mean Gaussian distributed with autocorrelation matrix $\mathbf{R}_\omega$. If $\mathbf{R}_\omega$ is independent of $\mathbf{h}$, the ML estimate can easily be determined.

In the problem under investigation, the autocorrelation matrix of the additive disturbance becomes independent of $\mathbf{h}$ only for the observation $\mathbf{r}_2$. Based on the observation $\mathbf{r}_2$, we can easily obtain the ML estimate of $\mathbf{h}$:

$$\hat{\mathbf{h}}_{\text{ML}} = (\mathbf{B}_2^+\mathbf{B}_2)^{-1}\mathbf{B}_2^+\mathbf{r}_2. \tag{26}$$

We call this the subset estimator, as only a subset of observations is used for the estimation. The mean-squared error of this estimate is given by

$$\text{MSE} = E\left[\left\|\mathbf{h} - \hat{\mathbf{h}}_{\text{ML}}\right\|^2\right] = \text{trace}\left(N_0(\mathbf{B}_2^+\mathbf{B}_2)^{-1}\right). \tag{27}$$

Hence, the MSE of this estimate reaches the subset GCRB which equals trace $(\mathbf{J}_2^{-1})$, that is, the estimate is a minimum variance unbiased (MVU) estimate. However, it should be noted that (27) is valid under the assumption $\mathbf{H}\mathbf{F}_d = \widetilde{\mathbf{F}}\widetilde{\mathbf{H}}$, which for finite block sizes is only an approximation. For finite block sizes, the observation $\mathbf{r}_2$ is affected by a residual contribution from the data symbols. In that case, the MSE of the estimate (26) is given by

$$\text{MSE} = \text{trace}\left(\mathbf{D}\mathbf{R}_{\widetilde{\mathbf{w}}}\mathbf{D}^+\right), \tag{28}$$

where $\mathbf{D} = (\mathbf{B}_2^+\mathbf{B}_2)^{-1}\mathbf{B}_2^+\mathbf{T}_2$ and $\mathbf{T}_2$ consists of the last M rows of $\mathbf{T}$. Note that the matrix $\mathbf{D}$ is proportional to $(E_s)^{-1/2}$. At low E_s/N_0, the autocorrelation matrix $\mathbf{R}_{\widetilde{\mathbf{w}}}$ converges to

$N_0\mathbf{I}_{N+\nu}$, in which case (28) converges to (27), which is inversely proportional to E_s/N_0. At high E_s/N_0, however, the residual contribution of the data symbols will be dominant, and the dominant part of $\mathbf{R}_{\widetilde{\mathbf{w}}}$ that contributes to (28) is proportional to E_s. Hence at high E_s/N_0 the MSE, (28) will become independent of E_s/N_0: an error floor will be present, corresponding to MSE = trace $(E_s(N/(N+\nu))\mathbf{D}\mathbf{H}\mathbf{F}_d\mathbf{F}_d^+\mathbf{H}^+\mathbf{D}^+)$. Note that the subset estimate (26) is only a true ML estimate as long as the assumption $\mathbf{H}\mathbf{F}_d = \widetilde{\mathbf{F}}\widetilde{\mathbf{H}}$ is valid; for finite block size, (26) is rather an ML-based ad hoc estimate.

As the transform $\mathbf{T}$ is obtained by the QR-decomposition of $\widetilde{\mathbf{F}}$, and $\widetilde{\mathbf{F}}$ is known when the positions of the data symbols are known, $\mathbf{B}_2$ only depends on the known pilot symbols and the known positions of the data carriers and the pilot carriers. Hence, $\mathbf{B}_2$ is known at the receiver and $(\mathbf{B}_2^+\mathbf{B}_2)^{-1}\mathbf{B}_2^+$ can be precomputed. Therefore, the estimate (26) can be obtained with low complexity.

4. NUMERICAL RESULTS

In this section, we evaluate the GCRBs obtained from the whole observation $\mathbf{r}_1$ and $\mathbf{r}_2$ (22) and the data-free observation $\mathbf{r}_2$ only (15). Without loss of generality, we assume the comb-type pilot arrangement [10] is used for the pilots transmitted on the carriers. We assume that the pilots are equally spaced over the carriers, that is, the positions of the pilot carriers are $I_p = \{n_0+m\epsilon \mid m = 0,\ldots,M-\nu-1\}$, where $\epsilon = \text{floor}(N/(M - \nu))$ and n_0 belongs to the set $\{0,\ldots,\rho\}$, with $\rho = (N-1)-(M-\nu-1)\epsilon$. Note however that the results can easily be extended for other types of pilot arrangements. From the simulations we have carried out, we have found that the equally spaced pilot assignment yields the best performance results. Further, we assume an L-tap channel with $h(\ell) = h(0)(L - \ell)$, for $\ell = 0,\ldots,L - 1$, which is normalized such that $\sum_{\ell=0}^{L-1}|h(\ell)|^2 = 1$; we have selected $L = 8$. The pilot symbols are BPSK modulated and generated independently from one block to the next. Unless stated otherwise, we compute the GCRB and the MSE for a large number of blocks and average over the blocks, in order to obtain results that are independent of the selection of the pilot symbols.

In Figure 2, we show the normalized GCRB, defined as CRB = $((N/(N+\nu))(E_s/N_0))^{-1}$ NCRB, as a function of the SNR = E_s/N_0 for the total observation $(\mathbf{r}_1, \mathbf{r}_2)$ and the subset $\mathbf{r}_2$ of observations only. Further, the low SNR limit trace $(N_0(\mathbf{B}^+\mathbf{B})^{-1})$ of the (G)CRB is shown. As expected, for low SNR (<-10 dB), the GCRB of the total observation coincides with the low SNR limit of the (G)CRB. At high SNR, the GCRB reaches the GCRB (27) for the subset observation. Further, it can be observed that the low SNR limit of the NCRB is essentially equal to L/M, as was shown in Section 2. Note that the difference between the low SNR limit and the high SNR limit is quite small (in our example the difference amounts to about 10%); this indicates that most of the estimation accuracy comes from the observation $\mathbf{r}_2$.

In Figure 3, the NCRB is shown as function of M for different values of the SNR. The (N)CRB is inversely proportional to M for a wide range of M. At low and high values of

M, the NCRB is increased as compared to L/M. This can be explained by Figure 4, which shows the influence of the pilot sequence on the GCRB. In this figure, the GCRB is computed for 50 randomly generated pilot sequences. Further, the average of the GCRB over the random pilot sequences is shown. Note that the GCRB depends on the values of the pilots through the first term in (22) only. At high values of M, the pilot spacing becomes $\epsilon = 2$ (for $N/4 < M - \nu < N/2 = 512$) and $\epsilon = 1$ (for $M - \nu > N/2 = 512$); in that case pilots are not evenly spread over the carriers but grouped in one part of the spectrum, and the approximation in the last line of (24) is no longer valid. This effect causes the peaks in the curve at high M. The GCRB in this case clearly depends on the values of the pilots: we observe an increase of the variance. The effect disappears when $M - \nu$ is close to $N/2 = 512$ or $N = 1024$: the spreading of the pilots over the spectrum becomes again uniform. Also at low values of M, the average value of the GCRB and the variance of the GCRB are increased. At low M, the contribution of the guard interval pilots is dominant. From simulations, it follows that this contribution strongly depends on the values of the pilots in the guard interval, and has large outliers when the guard interval pilots are badly chosen. Assuming the pilots in the guard interval are B-PSK modulated, the lowest GCRB in this case is achieved when the B-PSK pilots are alternating, that is, $\mathbf{b}_g = \{1, -1, 1, -1, \dots\}$. When M increases, the relative importance of the guard interval pilots reduces and the contribution of the pilot carriers becomes dominant. The GCRB turns out to be essentially independent of the values of the pilot carriers, as these pilots are multiplied with complex exponentials, which have a randomizing effect on the contributions of the pilot carriers. Hence, for increasing M, the GCRB becomes essentially independent of the used pilot sequence.

Figure 5 shows the dependency of the NCRB on the guard interval length for a fixed total number of pilots. It is observed that the NCRB slightly increases for increasing guard interval length. This can be explained by noting that when ν increases, the number of guard interval pilots increases while the number of pilot carriers decreases. Hence, when ν increases, the relative importance of the contribution of the guard interval pilots will increase. As shown in Figure 4, this will cause an increase of the GCRB. Hence, as the GCRB increases for increasing guard interval length when the total number of pilots is fixed, it is better to keep the guard interval length as small as possible (i.e., $\nu = L - 1$ in order to avoid intersymbol interference) and put the other pilots on the carriers.

The dependency of the GCRB on the FFT size N is shown in Figure 6. The GCRB is constant over a wide range of N. Only at low values of N, the GCRB slightly increases. Note that for low N, the approximations $\mathbf{HF}_d = \widetilde{\mathbf{F}}\widetilde{\mathbf{H}}$ and $\widetilde{\mathbf{F}}\widetilde{\mathbf{F}}^+ = \mathbf{I}_{N+\nu-M}$ do not hold, and the approximate analytical expression for the GCRB looses its practical meaning. However, for the range of N for which the derived approximation for the GCRB is valid, we can conclude that the GCRB is independent of N. This can intuitively be explained as follows. The FFT size N will mainly contribute to the GCRB through the data symbols $\mathbf{a}_d$, as the number of data symbols increases
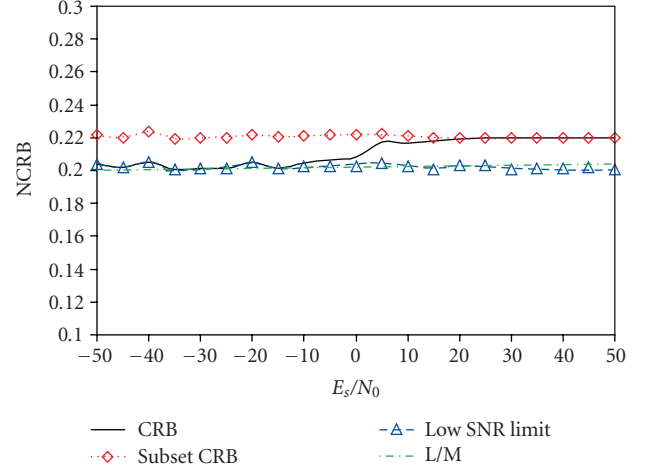

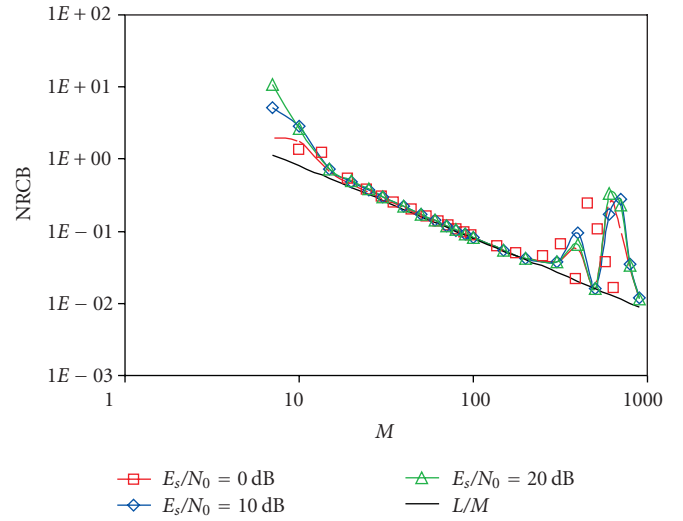FIGURE 2: Normalized GCRB, $\nu = 7$, $N = 1024$, $M = 40$.

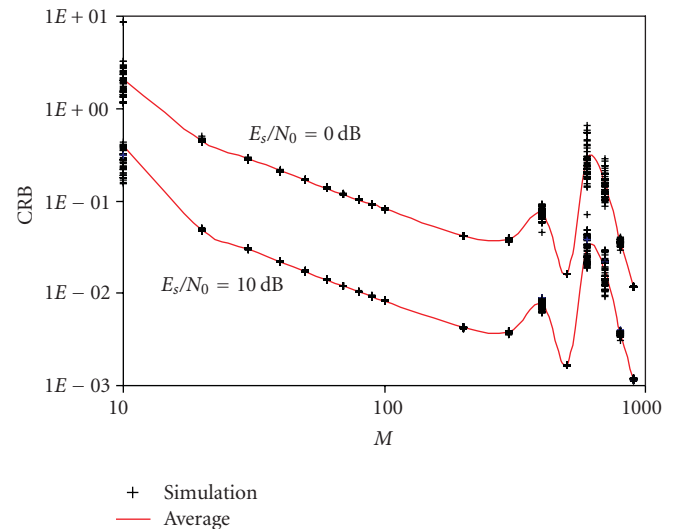FIGURE 3: Influence of the number of pilots M on the GCRB, $\nu = 7$, $N = 1024$.

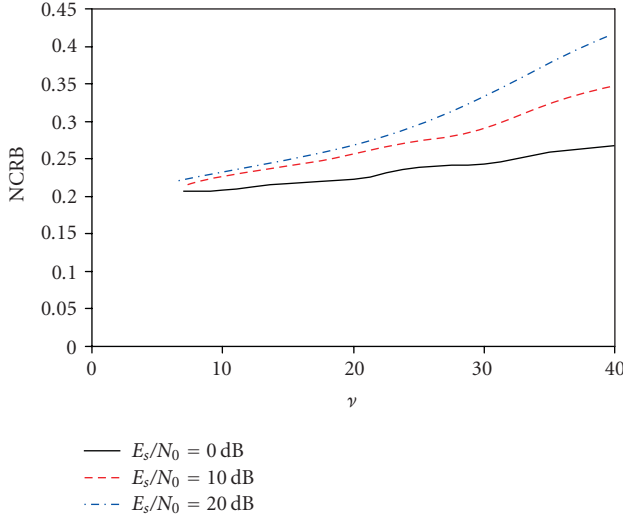FIGURE 4: Influence of the pilot sequence on the GCRB, $\nu = 7$, $N = 1024$.

FIGURE 5: Influence of the guard interval length ν on the GCRB, $M = 40$, $N = 1024$.
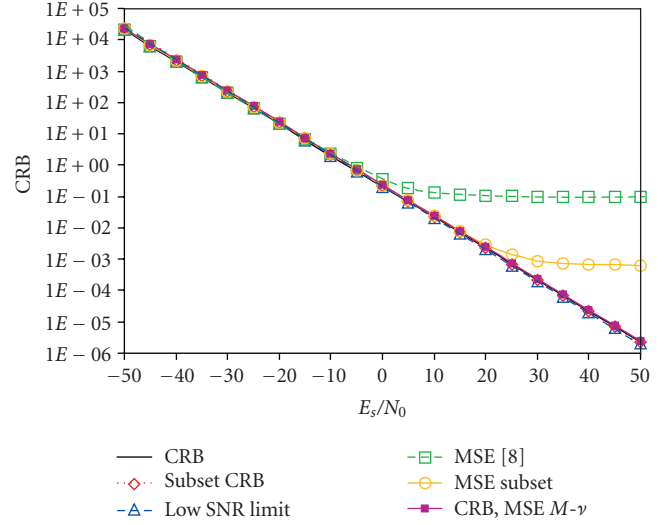

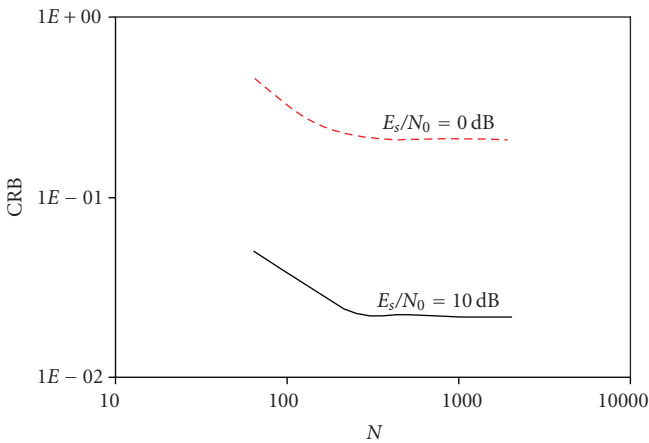FIGURE 7: GCRB and MSE, $N = 1024$, $M = 40$, $\nu = 7$.

FIGURE 6: Influence of the FFT length N on the GCRB, $M = 40$, $\nu = 7$.

with increasing N. However, we have shown that most of the estimation accuracy of the GCRB comes from the observation $\mathbf{r}_2$, which is the data-free part of the observation. Therefore, the presence of the data symbols will have almost no influence of the GCRB, resulting in the GCRB to be independent of N.

In Figure 7, we show the GCRB for both the total observation and the subset observation, along with the low SNR limit of the (G)CRB. Although it follows from Figure 2 that the GCRB and the subset GCRB are larger than the low SNR limit of the (G)CRB, the difference is small: the curves in Figure 7 are close to each other. In Figure 7, we also show the MSE (28) of the proposed subset estimator. As can be observed, the MSE coincides with the subset GCRB for a large range of SNR. Only for large SNR (>20 dB), the MSE shows an error floor as shown in the previous section, indicating that for $E_s/N_0 > 20$ dB the approximation $\mathbf{HF}_d = \widetilde{\mathbf{F}}\widetilde{\mathbf{H}}$ is no longer valid. Further, we show in Figure 7 the MSE of a sub-

optimal ML-based estimator for the channel, derived in [8] and based on the estimator given in [11]. In the latter estimator, it is assumed that the autocorrelation matrix $\mathbf{R}_{\widetilde{\mathbf{w}}}$ of the disturbance $\widetilde{\mathbf{w}}$ (6) is known. Assuming the autocorrelation matrix $\mathbf{R}_{\widetilde{\mathbf{w}}}$ does not depend on the parameters to be estimated (which is not the case), the latter estimator is derived based on the ML estimation rule. It is clear that the estimator proposed in this paper outperforms the estimator from [8]. Further, in the latter estimator the autocorrelation matrix $\mathbf{R}_{\widetilde{\mathbf{w}}}$ is in general not known but must be estimated from the received signal. Therefore, the complexity of the estimator from [8] is much higher than that of the proposed estimator, as in the former case, the autocorrelation matrix first has to be estimated from the received signal before channel estimation can be carried out.

5. CONCLUSIONS AND REMARKS

In this paper, we have derived an approximation (which is accurate for large block size) for the Cramer Rao bound, that is, the Gaussian Cramer-Rao bound, related to for data-aided channel estimation in KSP-OFDM, when the pilot symbols are distributed over the guard interval and pilot carriers. An analytical expression for the GCRB is derived by applying a suitable linear transformation to the received samples. It turns out that the GCRB is essentially independent of the FFT length, the guard interval, and the pilot sequence, and is inversely proportional to the number of pilots and to E_s/N_0. At low SNR, the GCRB obtained in this paper coincides with the low SNR limit of the true CRB, derived in [8]. At high SNR, the GCRB reaches the GCRB corresponding to the data-independent subset of the observation, indicating that at high SNR, observations affected by data symbols can be safely ignored when estimating the channel. Further, we have compared the MSE of the subset estimator with the obtained GCRB and with the MSE of the ML-based channel estimator from [8]. The proposed estimator coincides with the subset

GCRB for a large range of SNR. Only at large SNR, the MSE shows an error floor. However, the proposed estimator outperforms the estimator from [8], both in terms of complexity and performance.

In CP-OFDM, the N samples corresponding to the data part of the received signal are transformed to the frequency domain by an FFT, and the guard interval samples are not transformed. In ZP-OFDM, first the samples from the guard interval are added to the first v samples from the data part of the received signal, and then the N samples from the data part are applied to an FFT, while the guard interval samples are not transformed. In both cases, the used transform is an invertible linear transformation that is independent of the parameter to be estimated. As the different carriers do not interfere with each other, it can be shown that the FFT outputs corresponding to the pilot carriers contain necessary and sufficient information to estimate the channel. Therefore, the observations that are used to estimate the channel in CP-OFDM and ZP-OFDM are the FFT outputs corresponding to the pilot carriers; the observations corresponding to the data carriers and the guard interval samples are neglected. Hence, in CP-OFDM and ZP-OFDM channel estimation is performed in the frequency domain. As the FFT outputs at the pilot positions are independent of the transmitted data, the ML channel estimate and associate true CRB for CP-OFDM and ZP-OFDM are easily to obtain [8]. However, in KSP-OFDM, such a simple linear transformation cannot be found to obtain M observations independent from the data symbols, that is, the pilots are split over the guard interval and the carriers, and the data symbols interfere with the guard interval carriers. Therefore, channel estimation in KSP-OFDM is in general more complex than for CP-OFDM and ZP-OFDM.

APPENDIX

A. DETERMINATION OF J_1 (21)

Taking into account (18) and (19), the derivative of $\ln p(\mathbf{r}_1 \mid \mathbf{h})$ with respect to $h(k)$ is given by

$$\frac{d\ln p(\mathbf{r}_1 \mid \mathbf{h})}{dh(k)}$$
$$= \beta_k - (\mathbf{r}_1 - \mathbf{B}_1\mathbf{h})^+\mathbf{R}_1^{-1}\mathbf{B}_1\mathbf{1}_k + (\mathbf{r}_1 - \mathbf{B}_1\mathbf{h})^+\widetilde{\mathbf{Q}}_k(\mathbf{r}_1 - \mathbf{B}_1\mathbf{h}),$$
(A.1)

where

$$\widetilde{\mathbf{Q}}_k = (\widetilde{\mathbf{F}}^+\mathbf{T}_1^+)^{-1}\mathbf{X}_k(\mathbf{T}_1\widetilde{\mathbf{F}})^{-1},$$
$$\mathbf{X}_k = \mathrm{diag}\left(\frac{\gamma_{k,\ell}}{|\alpha_\ell|^2}\right);$$
(A.2)

$\mathbf{1}_k$ is a vector of length L with a one in the kth position and zeros elsewhere; and α_ℓ, $\gamma_{k,\ell}$, and β_k are defined as in (17),

(20). Hence, the elements of the Fisher information matrix $\mathbf{J}_1$ are given by

$$\begin{aligned}(\mathbf{J}_1)_{k,k'} &= (\mathbf{B}_1^+\mathbf{R}_1^{-1}\mathbf{B}_1)_{k,k'} + \beta_k^*\beta_{k'}\\ &+ \beta_k^*\mathrm{trace}(\widetilde{\mathbf{Q}}_{k'}\mathbf{R}_1) + \beta_{k'}\mathrm{trace}(\widetilde{\mathbf{Q}}_k^+\mathbf{R}_1)\\ &+ \mathrm{trace}(\widetilde{\mathbf{Q}}_k^+\mathbf{R}_1)\mathrm{trace}(\widetilde{\mathbf{Q}}_{k'}\mathbf{R}_1)\\ &+ \mathrm{trace}(\widetilde{\mathbf{Q}}_k^+\mathbf{R}_1\widetilde{\mathbf{Q}}_{k'}\mathbf{R}_1).\end{aligned}$$
(A.3)

Taking into account that $\mathbf{R}_1 = \mathbf{T}_1\widetilde{\mathbf{F}}\Delta\widetilde{\mathbf{F}}^+\mathbf{T}_1^+$, $\widetilde{\mathbf{Q}}_k = (\widetilde{\mathbf{F}}^+\mathbf{T}_1^+)^{-1}\mathbf{X}_k(\mathbf{T}_1\widetilde{\mathbf{F}})^{-1}$ and $\mathrm{trace}(\mathbf{XY}) = \mathrm{trace}(\mathbf{YX})$, it follows that $\mathrm{trace}(\widetilde{\mathbf{Q}}_k\mathbf{R}_1) = \mathrm{trace}(\mathbf{X}_k\Delta)$ and $\mathrm{trace}(\widetilde{\mathbf{Q}}_k^+\mathbf{R}_1\widetilde{\mathbf{Q}}_{k'}\mathbf{R}_1) = \mathrm{trace}(\mathbf{X}_k^+\Delta\mathbf{X}_{k'}\Delta)$. Further, note that $\Delta = \mathrm{diag}(\alpha_\ell)$, then it follows that

$$\mathrm{trace}(\widetilde{\mathbf{Q}}_k\mathbf{R}_1) = -2\beta_k^*$$
(A.4)

and

$$\mathrm{trace}(\widetilde{\mathbf{Q}}_k^+\mathbf{R}_1\widetilde{\mathbf{Q}}_{k'}\mathbf{R}_1) = \sum_{n_\ell\in I_d}\frac{\gamma_{k,\ell}^*\gamma_{k',\ell}}{|\alpha_\ell|^2}.$$
(A.5)

Substituting (A.4) and (A.5) in (A.3) yields (21).

B. DETERMINATION OF $\mathbf{J}$ (22)

Substituting (21) and (15) in $\mathbf{J} = \mathbf{J}_1 + \mathbf{J}_2$, it follows that the Fisher information matrix $\mathbf{J}$ can be written as

$$\begin{aligned}\mathbf{J}_{k,k'} &= (\mathbf{B}_1^+\mathbf{R}_1^{-1}\mathbf{B}_1)_{k,k'} + \frac{1}{N_0}(\mathbf{B}_2^+\mathbf{B}_2)_{k,k'} + \beta_k^*\beta_{k'} + \sum_{n_\ell\in I_d}\frac{\gamma_{k,\ell}^*\gamma_{k',\ell}}{|\alpha_\ell|^2}\\ &= ((\mathbf{TB})^+\mathbf{R}_{\mathbf{w}'}^{-1}(\mathbf{TB}))_{k,k'} + \beta_k^*\beta_{k'} + \sum_{n_\ell\in I_d}\frac{\gamma_{k,\ell}^*\gamma_{k',\ell}}{|\alpha_\ell|^2},\end{aligned}$$
(B.1)

where it was taken into account that

$$\mathbf{R}_{\mathbf{w}'} = \begin{pmatrix}\mathbf{R}_1 & \mathbf{0}\\ \mathbf{0} & \mathbf{R}_2\end{pmatrix},$$
(B.2)

$\mathbf{R}_2 = N_0\mathbf{I}_M$, and

$$\mathbf{TB} = \begin{pmatrix}\mathbf{B}_1\\ \mathbf{B}_2\end{pmatrix}.$$
(B.3)

Further note that $\mathbf{R}_{\mathbf{w}'} = \mathbf{TR}_{\widetilde{\mathbf{w}}}\mathbf{T}^+$ and the transform $\mathbf{T}$ is a unitary matrix. Then it follows that the first term in (B.1) can be rewritten as $(\mathbf{TB})^+\mathbf{R}_{\mathbf{w}'}^{-1}(\mathbf{TB}) = \mathbf{B}^+\mathbf{R}_{\widetilde{\mathbf{w}}}^{-1}\mathbf{B}$, resulting in (22).

REFERENCES

[1] J. A. C. Bingham, "Multicarrier modulation for data transmission: an idea whose time has come," *IEEE Communications Magazine*, vol. 28, no. 5, pp. 5–14, 1990.

[2] B. Muquet, Z. Wang, G. B. Giannakis, M. De Courville, and P. Duhamel, "Cyclic prefixing or zero padding for wireless multicarrier transmissions?" *IEEE Transactions on Communications*, vol. 50, no. 12, pp. 2136–2148, 2002.

[3] L. Deneire, B. Gyselinckx, and M. Engels, "Training sequence versus cyclic prefix—a new look on single carrier communication," *IEEE Communications Letters*, vol. 5, no. 7, pp. 292–294, 2001.

[4] R. Cendrillon and M. Moonen, "Efficient equalizers for single and multicarrier environments with known symbol padding," in *Proceedings of the 6th International Symposium on Signal Processing and Its Applications (ISSPA '01)*, vol. 2, pp. 607–610, Kuala-Lampur, Malaysia, August 2001.

[5] O. Rousseaux, G. Leus, and M. Moonen, "A suboptimal iterative method for modified maximum likelihood sequence estimation in a multipath context," *EURASIP Journal on Applied Signal Processing*, vol. 2002, no. 12, pp. 1437–1447, 2002.

[6] T. M. Schmidl and D. C. Cox, "Robust frequency and timing synchronization for OFDM," *IEEE Transactions on Communications*, vol. 45, no. 12, pp. 1613–1621, 1997.

[7] U. Mengali and A. N. D'Andrea, *Synchronization Techniques for Digital Receivers*, Plenum Press, New York, NY, USA, 1997.

[8] H. Steendam and M. Moeneclaey, "Different guard interval techniques for OFDM: performance comparison," in *Proceedings from the 6th International Workshop on Multi-Carrier Spread Spectrum (MC-SS '07)*, vol. 1, pp. 11–24, Herrsching, Germany, May 2007.

[9] H. L. Van Trees, *Detection, Estimation and Modulation Theory*, John Wiley & Sons, New York, NY, USA, 1968.

[10] F. Tufvesson and T. Maseng, "Pilot assisted channel estimation for OFDM in mobile cellular systems," in *Proceedings of IEEE 47th Vehicular Technology Conference (VTC '97)*, vol. 3, pp. 1639–1643, Phoenix, Ariz, USA, May 1997.

[11] O. Rousseaux, G. Leus, and M. Moonen, "Estimation and equalization of doubly selective channels using known symbol padding," *IEEE Transactions on Signal Processing*, vol. 54, no. 3, pp. 979–990, 2006.